Binary Shuffled Frog Leaping Algorithm for Optimal Allocation of Power Quality Monitors in Unbalanced Distribution System

Ashkan Doust Mohammadi, Mohammad Mohammadi

Abstract:

This paper deals with optimal detection of number and best locations of power quality monitors (PQMs) in an unbalanced distribution network based on the monitor reach area concept. The proposed model uses binary string, representing the installation mode of PQMs (Yes or No) in each bus of the network. In this paper, the binary version of shuffled frog-leaping algorithm (BSFLA), because of having the ability to improve the search capability with a fast convergence rate, is utilized for the optimization process. The overall cost function is formulated to optimize the two indices, which are the monitor overlapping index and sag severity index. The only optimization constraint in this problem is that the number of monitors that can detect voltage sags due to a fault at a specific bus must not be zero. In this study, DIGSILENT software is utilized for fault analysis while the optimization problem is handled by the BSFLA. To verify the proposed algorithm, the IEEE 34 Bus unbalanced distribution network is considered as a case study and results are compared to similar investigations so as to illustrate the effectiveness of the proposed algorithm.

Keywords: *Binary shuffled frog-leaping algorithm, Topological monitor reach area (TMRA), Power quality, Power quality monitoring*

1. Introduction

Active power distributions need to be monitored online. This must be performed correctly from the point of view of various power quality indices. Harmonic, voltage sag, voltage swing and other power quality indices must be measured. Voltage sags monitoring and its assessment gives information about the actual cause and source of voltage sags that can help power engineers mitigate such disturbances. Thus, to accurately monitor the overall system, power quality monitors (PQM) need to be installed at all buses in a power system, which is very costly and uneconomical planning [1]. Therefore, new optimal placement methods are required to determine the minimum number and the best locations of PQMs to ensure that through an efficient allocation approach, any event that leads to voltage sag is captured. A few optimal allocation techniques of PQMs have been reported in the last few years. Generally, the voltage sag monitor placement techniques comprise four fundamental methods, namely, monitor reach area (MRA), covering and packing (CP), graph theory (GT), and multivariable regression (MVR) [2]. Dong and Seung proposed a new GT-based algorithm to monitor the voltage sag in a power system which represents the power system network using a simple graph with an incidence matrix and analyzed the system in a network matrix frame [3]. The GT-based topological technique based on coverage matrix was utilized for PQM placement by Dong and Seung [4]. In [5], a novel power quality monitoring allocation algorithm based on the CP method was discussed. In [6], a combinatorial problem of the CP method with the Integer Linear Programming (ILP) technique was employed to minimize the cost of PQMs. In [7], a method was presented by authors for the optimal placement of PQMs that is planned based on the CP approach and that used GAMS software to simulate the faults on the system. The CP method has two drawbacks. One is evaluating the system's connectivity to analyze system observability based on Kirchhoff's current and Ohm's law, and the second is considering steady state information in comparison with the actual information of voltage sag as constraints of the optimization problem. In 2011, a new method based on the MVR model was presented in the placement of PQMs [8]. A novel PQM placement technique using Cp and Rp statistical indices for power transmission and distribution networks was analyzed [9]. Recently, the MVR method was combined with Cp and Rp statistical indices and used for optimal PQM placement [10]. In recent years, the heuristics approaches have been mixed with the Cp statistical index approach to find the best location and improve the accuracy of the solution. For example, optimal power quality monitor placement in transmission networks using genetic algorithm and Mallow's Cp was addressed by [11]. Also, a similar study by the same authors was reported about optimal power quality monitor placement using the GA_Cp method for distribution network [12]. In 2003, Olguin et al. proposed a monitor reach area or MRA concept-based method, which gives the area of the network that can be observed from a given meter position by constructing a binary matrix. According to their proposed method, if a fault occurs inside MAR, then the event will trigger the PQM, while, for faults outside it, no PQM was triggered [13].

Thus, the MRAs of all possible locations using the binary MRA matrix through network faults located along the electrical lines are determined to establish and formulate the optimization problem. In MRA-based methods, the heuristics optimization algorithms are employed to determine the number of PQMs and best locations through optimizing objective function, which is formulated base on the MRA matrix. Many studies have been reported that used the MRA method combined with heuristics algorithms for optimal placement of PQMs. In [14], authors presented a method based on the concept of the MRA and the sag severity index for the placement of PQMs which used GA to solve the optimization problem. In the recently reported study, the concept of fuzzy, which was used in [15] is utilized for fuzzy monitor reach area (FMRA) to locate PQMs in large transmission network. The improved adaptive genetic algorithm (IAGA) was presented by [16] for optimal allocation of PQMs based on the MRA and MRM matrices and redundant vector concepts. Although the PQMs location in transmission systems using the MRA matrix technique is a simple performance, the MRA matrix is generally not suitable for application in radial distribution systems, as it often yields one PQM placement solution. Thus, in 2011, Ahmad Ibrahim proposed the new concept of topological monitor reach area (TMRA) and used it for optimal placement of PQMs in distribution systems [17]. The mentioned paper used the DIGSILENT software for fault analysis, while the optimization problem was handled by the GA. The TMRA was proposed not only to make observability applicable for transmission systems, but also for radial distribution systems. In TMRA, to ensure more flexibility of the search algorithms in consenting to sensitivity and economic capability, the alpha as the monitor coverage control parameter is implemented and added to MRA method. Authors in [18] solved the optimal power quality monitor placement in power systems based on TMRA using particle swarm optimization (PSO) and an artificial immune system (AIS). The quantum inspired particle swarm optimization (QPSO) was introduced by the same authors for PQM placement [19]. The adaptive QPSO (AQPSO) was also addressed for PQM placement based on MRA approach [20]. The first innovation of this study is using the DIGSILENT software combined with the MATLAB program for the unbalanced short circuit process. This technique increases the speed run of simulation. The second innovation uses the binary format of the shuffled frog-leaping based optimization algorithm to solve this problem (PQM placement). This aspect of the study was not performed by the others.

The main sections of this paper are listed as follows:

Section 2: Power Quality Monitor/Meters (Functions and Installation)

Section 3: Fundamental concepts about the residual fault voltage matrix, monitor reach area, system topology and topology monitor reach area.

Section 4: Objective function, illustrate the minimizing the number of required monitors (NRM), minimizing the monitor overlapping index (MOI) and maximizing the sag severity index (SSI).

Section 5: Optimization techniques, imperialist competitive approach and its binary version.

Section 6: Simulation and Results

Section 7: Conclusion

2. Power Quality Monitor/Meters (Functions and Installation)

The PQM is an ideal choice when continuous monitoring of a three phase system is required. It provides metering for current, voltage, real and reactive power, energy use, cost of power, power factor and frequency. In Figure 1, the schematic and installation of several types of PQM is presented. PQM's application and the monitoring and metering function of a typical type are listed as follows:

- Applications

1-Metering of distribution feeders, transformers, generators, capacitor banks and motors
2-Medium and low voltage systems
3-Commercial, industrial, utility
4-Flexible control for demand load shedding, power factor, etc.

- Monitoring and Metering

1-Harmonic analysis through 63rd with THD and TIF
2-Event recorder,
3-Waveform capture/4-Data logger

Figure 1. Schematic and installation of PQM

3. Fundamental Concepts

The main structure of the optimal PQM placement problem using the proposed approach is to understand the monitor observability concept. This structure is needed to explain the following concepts, which are discussed earlier in sections 3.1 to 3.4:

- Residual Fault voltage matrix

- Monitor reach area

- System topology

- Topology monitor reach area

3.1. Fault Voltage (FV) Matrix

In the MRA-based approach of PQM placement, the residual voltages at each bus of a system for all types of fault (single line to ground (SLG), two phases to ground (LLG), three phase faults (LLL)) and for all fault cases are required. In short circuit analysis, all types of faults are simulated, generally using the DIGSILENT software at each bus with zero fault impedance to form the FV matrix.

It is clear the worst fault with severe and critical results is the fault with minimum impedance. In the single phase to ground and three phases to ground faults, if the impedance of the point fault to ground experiment is the zero value, the largest current fault will be achieved. Therefore, it is better to design the system under the worst fault with the largest fault current. The design of system with PQMs under this condition can guarantee the good performance of the system for other conditions of fault. This note is illustrated in the revised paper. In the unsymmetrical faults for example in the single to ground fault (SLG), we have:

$$I_F^+ = I_F^- = \frac{E_{th}^{p.u} = 1}{X_{th}^+ + X_{th}^- + X_{th}^0 + X_F}, \ I_F^0 = 0 \quad (1)$$

In which, X_F denotes the fault impedance (reactance) at the fault point (fault to ground) and X_{th}^+, X_{th}^- and X_{th}^0 denote the positive, negative and zero sequences equivalent Thevenin impedances from the fault point which affected by topology of system. The smaller the X_F, the higher the positive and negative sequence fault currents I_F^+, I_F^-, and so we have higher fault currents of phases a, b and c (I_A^F, I_B^F and I_C^F).

$$\begin{bmatrix} I_A^F \\ I_B^F \\ I_C^F \end{bmatrix} = \begin{bmatrix} 1 & 1 & 1 \\ 1 & 1\angle -120 & 1\angle +120 \\ 1 & 1\angle +120 & 1\angle -120 \end{bmatrix} \times \begin{bmatrix} I_F^0 \\ I_F^+ \\ I_F^- \end{bmatrix} \quad (2)$$

Finally, the residual voltages as FV matrix are kept to employ in MRA formulation. In the FV matrix, the matrix column (j) is related to bus numbers of residual voltages, and its row (k) is correlated to the position of the simulated fault for a specific fault type [17, 21]. To better understand the concept of FV, consider a simple power system shown in Figure 2.

During a specific fault at bus 3, the voltage readings at each bus of the system are computed using DIGSILENT. These voltage values correspond to the 3rd row of the constructed FV matrix for the system, which is reported for a complete fault analysis of the system as in Figure 3.
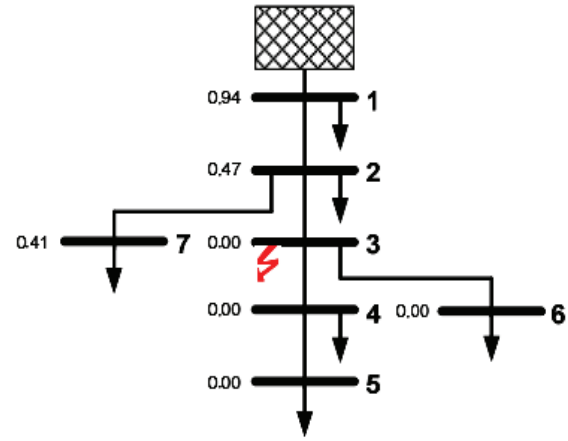

Figure 2. A simple radial distribution system

Figure 3. An example of the FV matrix

The residual voltage at each bus is valuable information in the formation of the monitor reach area (MRA). Therefore, it is necessary to store the residual voltages in a matrix called the Fault Voltage (FV) matrix, where the matrix columns represent the bus number and the matrix rows relate to the simulated fault position. Then, the MRA matrix can be obtained by comparing all the FV matrix elements for each phase with a threshold value. Each element of the MRA matrix is filled with 1 (one), when the bus residual voltage goes below or equal to α p.u. in any phase and with 0 (zero) otherwise. In the step of the short circuit process about fault analysis, it is necessary to simulate all the various kinds of fault. This step is performed generally at each bus using the DIGSILENT software without fault impedance (i.e., zero amount for it) to form and conclude the FV matrix. Finally, the residual voltages of the FV matrix are kept to employ in MRA formulation. (See Figure 11 for simulation of the short circuit analysis with DIGSILENT software and calculate the FV matrix).

3.2. Monitor Reach Area (MRA) Matrix

The concept of MRA can be explained as an area of the network that any fault that leads to voltage sag can be captured by a specified monitor location [22]. This MRA is a binary matrix where the MRA(j, k) = 1, signifies that point k is seen and covered by the installed PQM at bus j whereas MRA(j, k) = 0 identifies that point k is outside of the coverage area of the installed PQM at bus j. Any element of the MRA matrix can be obtained by comparing all the FV matrix elements for each phase with a threshold value which is represented by α parameter.

$$\begin{pmatrix} 1 & 1 & 1 & 1 & 1 & 1 & 1 \\ 1 & 1 & 1 & 1 & 1 & 1 & 1 \\ 0 & 1 & 1 & 1 & 1 & 1 & 1 \\ 0 & 1 & 1 & 1 & 1 & 1 & 1 \\ 0 & 0 & 1 & 1 & 1 & 1 & 1 \\ 0 & 1 & 1 & 1 & 1 & 1 & 1 \\ 0 & 1 & 1 & 1 & 1 & 1 & 1 \end{pmatrix}$$

Figure 4. An example of the MRA matrix

If the bus residual voltage of the FV matrix is less than or equal to α p.u. in any phase, then $MRA(j, k) = 1$, and otherwise, i.e., residual voltage of FV matrix is more than α p.u. at all phases, then $MRA(j, k) = 0$ as expressed follows:

$$MRA(j, k) = \begin{cases} 1 & \text{if FV(j,k)} \leq \alpha \text{ p.u at any phase} \\ 0 & \text{if FV(j,k)} > \alpha \text{ p.u at all phases} \end{cases} \quad (3)$$

To better understand the concept of the MRA matrix, consider the simple radial distribution system as shown in Figure 2 and its FV matrix obtained in Figure 3. In this example case, the threshold is set at $\alpha = 0.9$ p.u., the formation of the MRA matrix-based equation (3) and the yields MRA matrix as shown in Figure 4.

3.3. System Topology Matrix (T)

Like to MRA and FV matrices, the T matrix column is related to bus number and its row corresponds with fault location. When there is a path from generator bus to a particular bus in the system, the matrix is filled with 1 (one) and otherwise filled with 0 (zero) [23]. When a fault occurs in a particular bus, namely a faulted bus, it becomes a cut vertex that splits into various vertices of the same component as many adjacent edges. Some examples of a particular row in a T matrix for a single fed radial system, a doubly fed radial system, and a ring system are presented in Figure 5. For instance during fault at bus 3, depending on the number of feeders connected to this bus, the system graph will be separated into several sections. By checking the connectivity status between generator bus and the other bus based on mentioned criteria the T matrix elements are then filled with '1' or '0'. As shown in Figure 5, (a) the system has only one power source at bus 1. Clearly, there is a path from the generator bus (bus 1) to buses 1, 2, and 3 but not for the rest. Therefore, T matrix elements are filled with '1' up to column three and '0' for the rest. As indicated in Figure 5(b), in this case, the bus numbers 4 and 5 have been connected to the second power source and thus, the T matrix is filled with '1' up to column 5. In the last case, a ring system, as shown in Figure 5(c), gives all '1's for the T matrix column because of connections between the generator bus (bus 1) and the other buses. These examples are designed with a fault only at bus 3, and it needs to be similarly repeated on all
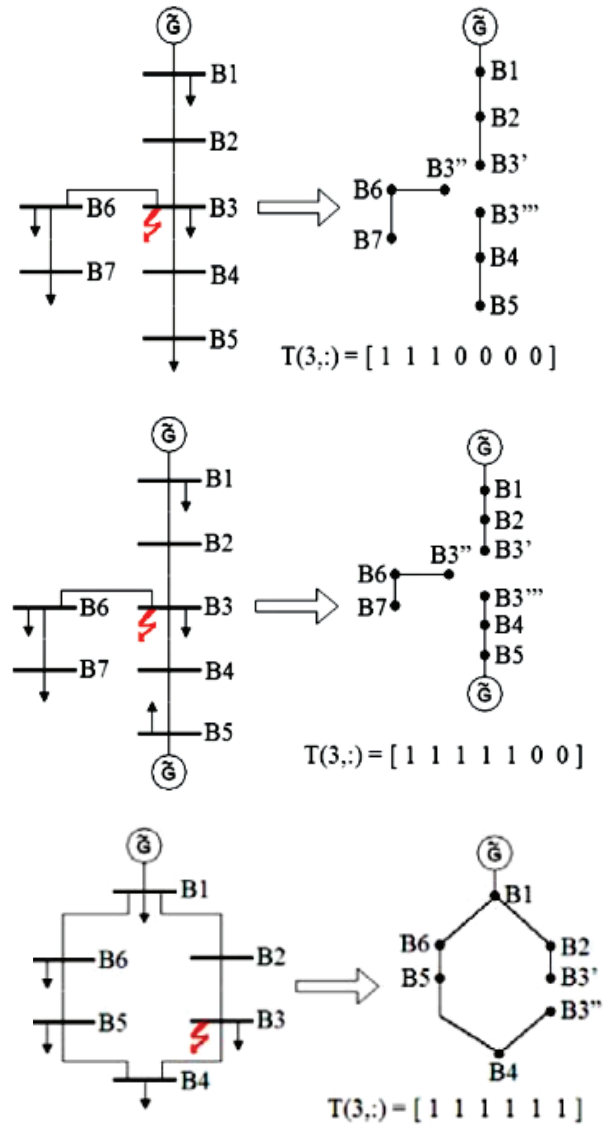
Figure 5. Example of row 3 in T matrix for different system topologies [22]

buses to give the information about system topology through a complete T matrix.

3.4. Topology Monitor Reach Area Matrix (TMRA)

The topological monitor reach area (TMRA) is introduced to make it applicable for both distribution and transmission systems. The TMRA matrix is a combination of MRA matrix and system topology (T) matrix by using operator 'AND' as expressed in (4) [17].

$$TMRA(j, k) = MRA(j, k) \bullet T(j, k) \quad (4)$$

4. Problem Formulation

The three main parts of a typical optimization problem are decision vector, objective function and constraints. Therefore, each item has been illustrated in regard to optimal solution of PQM placement.

4.1. Decision Vector

The decision vector that represents the Monitor Placement (MP) vector is introduced as a binary decision vector in bits in the optimization process.

Each bit indicates the positions of monitors that are installed or not in power system network. If $MP(n) = 1$, it indicates that a sag monitor should be installed at bus n whereas a value 0 means that no monitor needs to be installed at bus n. This MP vector can be described as follows [20]:

$$MP(n) = \begin{cases} 1 & \text{if monitor is required at bus } n \\ 0 & \text{if monitor is not required at bus } n \end{cases} \quad (5)$$

4.2. Objective Function

The PQM optimization problem discussed in this study deals with three objective functions that are addressed follows.

1. Minimizing the number of required monitors (NRM)

The first objective function is to minimize the number of required monitors (NRM), which can easily be obtained as expressed in (6), and this parameter needs to be minimized.

$$NRM = \sum_{n=1}^{N_{bus}} MP(n) \quad (6)$$

2. Minimizing the monitor overlapping index (MOI)

Monitor overlapping index (MOI) is introduced to assess the best monitor organization in a power system. Overlaps of monitor coverage areas for different arrangements are the issue of PQM placement in a power system. Here, it is essential to consider that these overlaps represent the number of sag monitors that report the same fault happening in a power system. Thus, these overlaps should be minimized. The overlaps can be determined by multiplying the TMRA matrix and the transposed MP vector. If all the elements in the obtained results are 1, it signifies that there isn't any overlap of the monitors' coverage. A lower MOI index represents a better organization of PQMs in a power system [19].

The MOI is given by:

$$MOI = \frac{\sum(TMRA * MP^T)}{NFLT} \quad (7)$$

Where NFLT indicates the total number of fault locations considering all types of faults.

3. Maximizing the sag severity index (SSI)

If several monitor configurations have the same MOI values, then in the evaluation step of monitor placement, the use of another index, which is called the Sag Severity Index (SSI), will be necessary. This index signifies the severity level of a particular bus regarding voltage sag where any fault that happens at this bus will make a serious drop in voltage magnitude in most buses of the system.

Thus, it is needed to calculate the severity level (SL) first. The SL is the total number of phases faced with voltage sags (NSPB) with magnitudes below t p.u. considering the number of phases in total for the system (NTPB) the SL is extracted as below [23]:

$$SL^t = \frac{\sum N_{SPB}}{\sum N_{TPB}} \quad (8)$$

Finally, the SSI is determined by weighting coefficients which applied for different severity levels. It is notable that the lowest t value is appointed with the maximum weighting factor and vice versa. In this study, five thresholds are considered; 0.1, 0.3, 0.5, 0.7 and 0.9 p.u.

$$SSI^F = \frac{1}{15} \sum_{k=1}^{5} k * SL^{\left(1 - \frac{2k-1}{10}\right)} \quad (9)$$

Finally, the computed SSI value must be stored in a matrix form where the matrix column is correlated to the bus number, and the matrix row is correlated to the type of fault (F). A higher value of SSI indicates a better placement of the monitor. The highest value of SSI at a particular bus implies that the bus is the most influential bus that causes voltage sag in a power system, and therefore, this bus needs to be given priority in installing a PQM compared to other buses with lower SSI values. In order to combine the MOI and SSI indices, both of them should have same optimal criteria of either maximum or minimum. In our study, the SSI matrix should be revised to conclude minimum value in optimization as the case of MOI. It is worth to note that the highest value of SSI matrix elements is equal to 1. SO, the suitable index can be extracted by the use of complementary matrix of SSI. As a result, a negative severity sag index (NSSI) is proposed to assess the best placement of PQMs. The NSSI can be determined by multiplying of complementary of SSI matrix with transposed MP vector with considering the number of fault types (NFT) as expressed follows [9]. Then a lower NSSI value concludes a better organization of PQMs.

$$NSSI = \frac{\sum[(1 - SSI) * MP^T]}{NFT} \quad (10)$$

Since the three mentioned objective functions have the same optimal criteria, with combination of them, the single objective function for minimization of the proposed problem is extracted as follows:

$$f = (NRM * MOI) + NSSI \quad (11)$$

4.3. Optimization Constraint

The only optimization constraint in this problem is that the monitoring times of the specific fault point must not be zero. It is important to note that the number of monitors that can detect voltage sags due to a fault at a particular bus can be obtained by the multiplication of the TMRA matrix by the transposed MP matrix. So his constraint is formulated as follows [22]:

$$\sum_{i=1}^{N} TMRA(n, i) * MP(i) \geq 1 \quad \forall n \quad (12)$$

5. Shuffled Frog-Leaping Algorithm

5.1. Classical Approach

The SFLA was originally introduced as a population-based meta-heuristic by M. Eusuff and K. Lansey [24]. This algorithm is inspired by the frog's life as a group when the frogs are in search of food. A shuffling strategy provides the mechanism to exchange information between local groups for the purpose of moving the solution towards a global optimum [25]. The term frog in SFLA is similar to chromosome in Genetic Algorithm (GA) or particle in Particle Swarm Optimization (PSO) approach. In SFL, the population of the frogs (solutions) is divided into different groups referred to as *memeplexes*.

The steps of the algorithm are as follows:

Initializing the population: Create an initial population of **P** frogs generated randomly, P={X_1, X_2, ..., X_P} which for **z**-dimensional problems (**z** variables), the position of *ith* frog in the search space is represented as $x_i = [x_{i,1}, x_{i,2}, ..., x_{i,z}]$. A fitness function is defined to evaluate the frog's position. The frogs are then sorted in descending order in accordance with their fitness.

Partition frogs into memeplexes: Divide the frogs into m_p memeplexes each holding n_f frogs such that $P = m_p \times n_f$. The division is done with the first frog going to the first memeplex, the second one going to the second memeplex, the ith frog go to the ith memeplex and the $(i + 1)^{th}$ frog back to the first memeplex.

Local exploration: In this step, a process is applied to improve only the frog with the worst fitness (not all frogs) in each cycle. For each memeplex **k**, the frogs with the best and worst fitness are identified as $x_{best,k}$ and $x_{worst,k}$ respectively. Also, the frog with the global best fitness x_{gbest} is identified among all the memeplexes. For the memeplex **k** at the time or iteration **t**, the worst frog $x_{worst,k}$ leaps toward the best frog $x_{best,k}$ and the position of the worst frog is updated based on the leaping rule, as follows:

$$x_{worst,k}^t = x_{worst,k}^{t-1} + d_k^t \qquad (13)$$

$$\mathbf{d_k^t} = rand(x_{best,k}^{t-1} - x_{worst,k}^{t-1}) \qquad (14)$$

Where **t** is the current iteration number and $d_k = [d_{k,1}, d_{k,2}, d_{k,3}, ..., d_{k,z}]$ with $-D_{max} \leq d_{k,j} \leq D_{max}$, which D_{max} is the maximum allowed change of frog's position in one jump. If this process produces a better solution, it is replaced for the worst frog. Otherwise, the calculations in equations (13) and (14) are repeated but with respect to the global best frog (i.e. $x_{best,k}$ is replaced by x_{gbest}). If no improvement is possible, then a new solution is randomly generated to replace the worst frog. Based on Figure 6, the evolution process is continued for a specific number of iterations [30]. The steps of Figure 6 are listed as follows:

- Continue the calculation of step 3 for a specific number of iterations

- Reshuffie the frogs and sort them again.
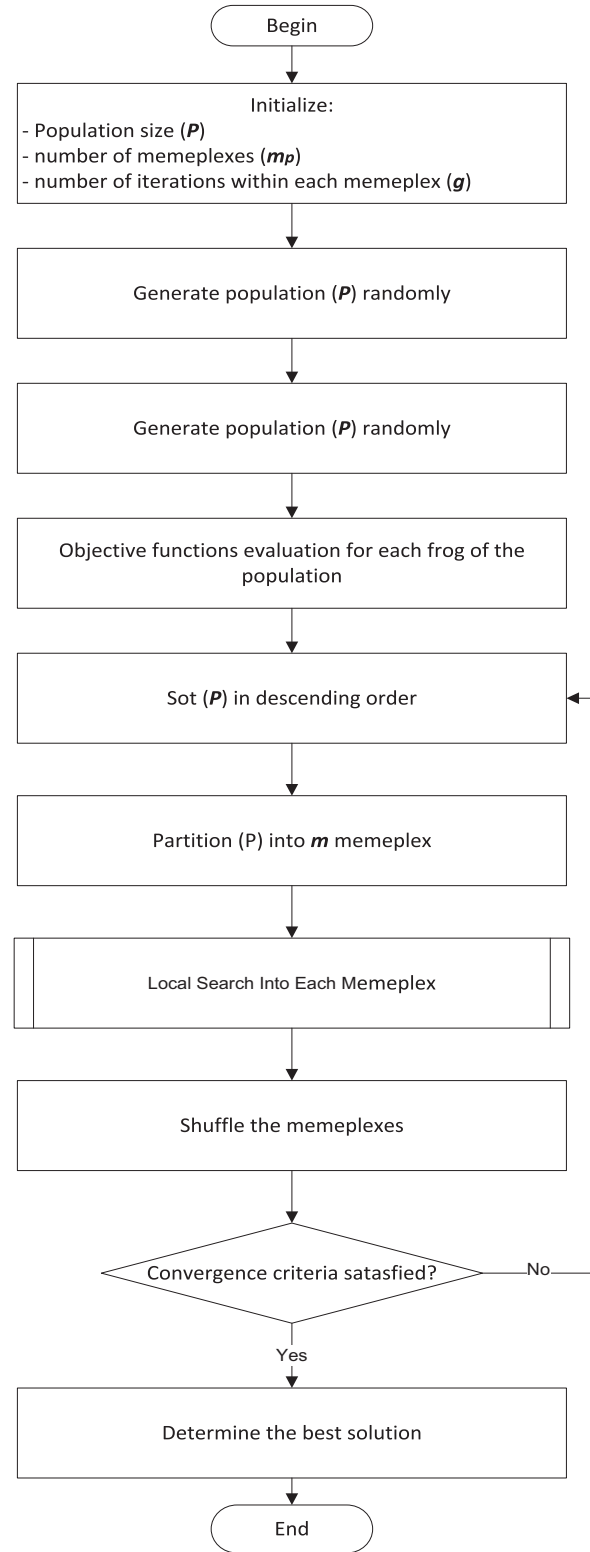
Figure 6. Flowchart of the BSFL algorithm

- Return back to step 2, if the termination criterion is not met, else stop.

Accordingly, the main parameters of SFL are: number of frogs, **P**; number of memeplexes m_p; number of frogs in each memeplex, n_f; number of generations for each memeplex before shuffling, **g**; number of shuffling iterations; number of shuffling iterations, t_{max}. In Figure 7, the flowchart of local search as a part of Figure 6, is presented.

```
                    ┌─────────────┐
                    │    Begin    │
                    └─────────────┘
                           │
                           ▼
              ┌──────────────────────────┐
              │  First memeplex, k=1     │
              └──────────────────────────┘
                           │
                           ▼
         ┌───────────────────────────────────────┐
         │ Determine Xbest,k, Xworst,k and Xgbest │◄──┐
         └───────────────────────────────────────┘   │
                           │                          │
                           ▼                          │
              ┌──────────────────────────┐            │
              │  First iteration, t=1    │            │
              └──────────────────────────┘            │
                           │                          │
                           ▼                          │
         ┌─────────────────────────────────┐          │
    ┌───►│  Apply equations (13) and (14)  │          │
    │    └─────────────────────────────────┘          │
    │                      │                           │
    │                      ▼                           │
    │               ╱────────────╲                     │
    │        Yes   ╱ Is Xworst,k  ╲                    │
    │      ┌──────◄  new is better  ►                  │
    │      │       ╲ than Xworst,k?╱                   │
    │      │        ╲────────────╱                     │
    │      │              │ No                         │
    │      │              ▼                            │
    │      │   ┌──────────────────────────────┐        │
    │      │   │ Geneae Xworst,k at iteration │        │
    │      │   │        t randomly            │        │
    │      │   └──────────────────────────────┘        │
    │      │              │                            │
    │      │              ▼                            │
    │      │   ┌──────────────────────────┐            │
    │      └──►│         t=t+1            │            │
    │          └──────────────────────────┘            │
    │                     │                            │
    │                     ▼                            │
    │              ╱────────────╲                      │
    │      Yes    ╱   t ≤ g?     ╲                     │
    └────────────◄                ►                    │
                  ╲────────────╱                       │
                        │ No                           │
                        ▼                              │
             ┌──────────────────────┐                 │
             │   Next memeplex      │─────────────────┘
             └──────────────────────┘
                        │
                        ▼
                 ╱────────────╲
                ╱   k ≤ mp     ╲    Yes
               ◄                ►────────┐
                ╲────────────╱           │
                        │ No             │
                        ▼                │
                 ┌─────────────┐         │
                 │     End     │         │
                 └─────────────┘         │
```
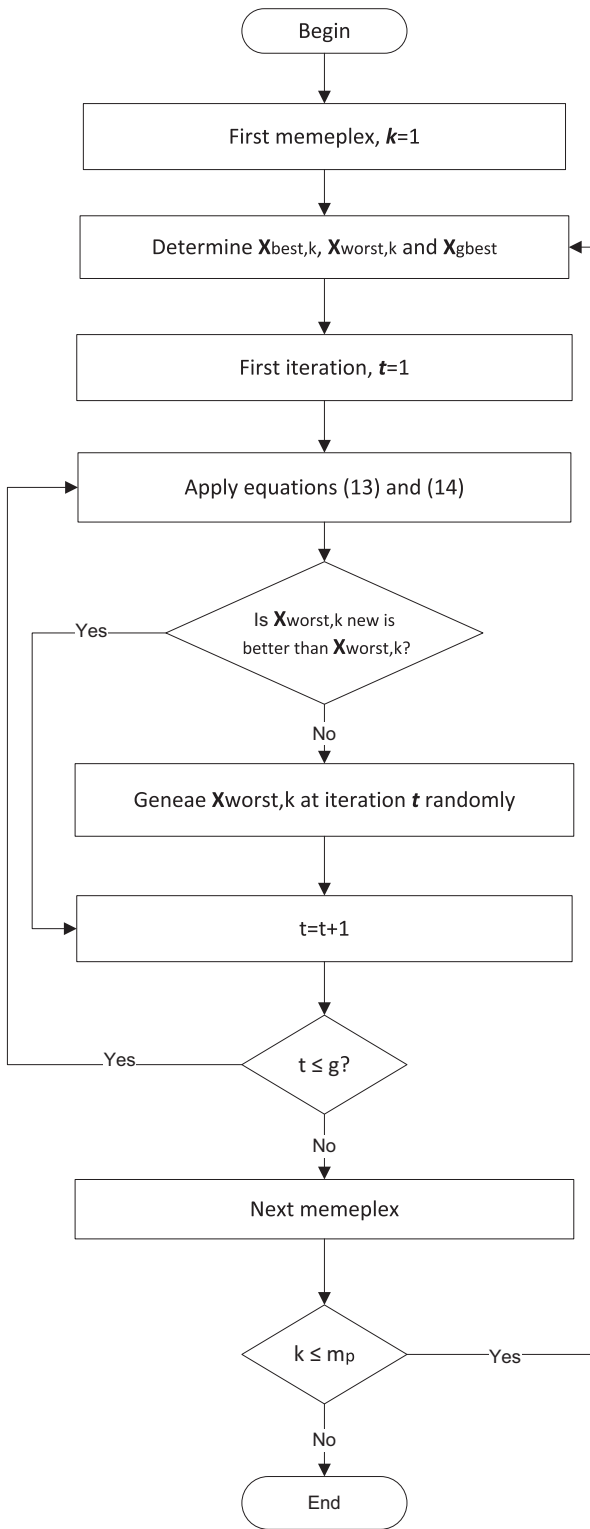
Figure 7. Flow-chart of the local search into each memeplex

5.2. Binary Shuffled Frog-Leaping Algorithm (BSFLA)

In discrete binary search space, every position vector can take only 0 or 1. The movement means that the corresponding variable value changes from 0 to 1or vice versa. In order to propose a binary version of the SFL, it is required to modify the some fundamental concepts of SFL. The leaping rule of the frogs maybe considered similar to the continuous algorithm (11).
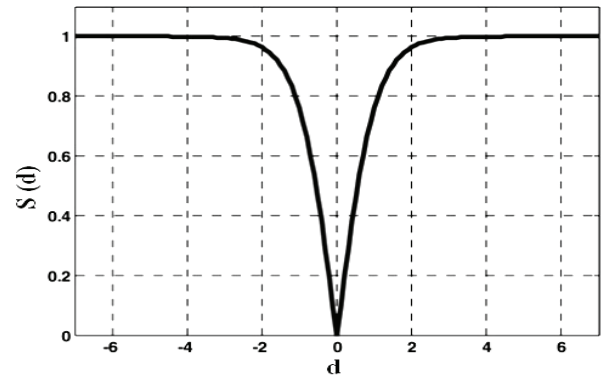

Figure 8. Probability function

The main aspect that distinguishes the binary SFL (BSFL) from classical SFL is that in the binary version, the making update of the worst position means the switching between '0' and '1' values. This switching should be performed in accord with the leaping rule. The idea is to make the position update in such a way that the BSFL changes the current bit with a probability value which is determined in accord with the leaping rule. This means that, BSFL updates the leaping rule and considers the new worst position to be either 1 or 0 with a given probability. To introduce a suitable transfer function to make a relation between the leaping rule and the probability updating of worst position, two basic concepts must be considered.

† When the current position of the worst solution is not proper so a great absolute jump is needed to arrive the best position and as a result changing the position of the worst solution must be provided with a high probability.

† When the current position of the worst solution is close to the best position so a small absolute jump is needed to get the best position and as a result changing the position of the worst solution must be provided with a low probability close to zero. Thus considering above points, for a small $|d_k^t|$, the probability of movement xworst,k must be near zero and for a large $|d_k^t|$ the probability of changing xworst,k must be high. To overcome this problem the function $S(d_k^t)$ based on absolute "tanh" transformation to the component of absolute jump is presented as follows [26].

$$S(d_k^t) = |\tanh(d_k^t)| = \left| \frac{\exp(2|d_k^t|) - 1}{\exp(2|d_k^t|) + 1} \right| \quad (15)$$

$S(d_k^t)$ squashes absolute jump into the range of [0, 1] and increases with increasing $|d_k^t|$ as shown in Figure 8. Once $S(d_k^t)$ is computed, the movement of frogs will be done as follows:

$$\begin{cases} 1: \text{i.e.} \rightarrow x_{worst,k}^t = x_{worst,k}^{t-1} + d_k^t & if\ rand < S(d_k^t) \\ 0: \text{i.e.} \rightarrow x_{worst,k}^t = x_{worst,k}^{t-1} & else \end{cases}$$
$$(16)$$

To get a pleasant convergence rate, the frogs jump must limit as $|d_k^t| \leq D_{max}$ which based on experiments, D_{max} is better set to be 6.

5.3. BSFLA for Optimal PQM Placement

Using the BSFLA, an algorithm for the optimal placement of PQMs can be obtained:

Step 1: Power flow and short circuit analyses are implemented.

Step 2: SL is calculated, and an SSI matrix is formed. The MRA matrix is constructed simultaneously based on the short circuit results.

Step 3: The **T** matrix is developed from the network configuration, and the TMRA matrix is constructed.

Step 4: All entries of the MP vectors (frog's positions, x_{ij}) in the system are randomly initialized.

Step 5: If the MP vectors don't fulfill the mentioned constraints, the entries of each MP vector are manipulated to fulfill the constraints.

Step 6: All the PQM placement evaluation indices, namely, NRM, MOI, and NSSI, are obtained.

Step 7: The performance of each MP vector is evaluated with the formulated objective function (f) based on the obtained indices. The fitness values for each frog, $f_i(t)$, are recorded.

Step 8: The frogs are then sorted in descending order in accord with their fitness.

Step 9: Partitioning frogs into memeplexes was performed using divide the frogs into m_p memeplexes each holding n_f frogs.

Step 10: Local exploration as a process is applied to improve only the frog with the worst fitness (not all frogs) in each cycle and the position of the worst frog is updated based on the leaping rule.

Step 11: Each MP vector to a new position is updated with criteria presented in (Eq. 13) and (Eq. 14).

Step12: Steps 5–12 are repeated until convergence is obtained, where the best fitness value is equal to the worst fitness value. Up on convergence, the optimal PQM placement is obtained.

The overall procedure in the optimal PQM placement method using BSFLA is shown in a flowchart in Figure 9.
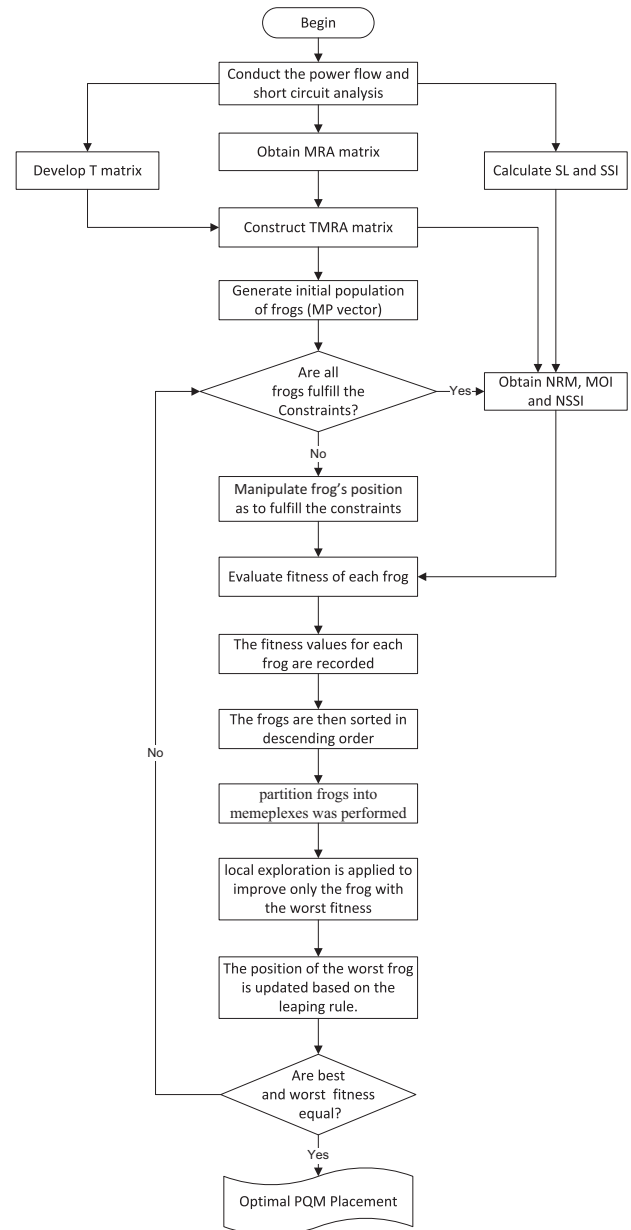
6. Simulation and Results

The IEEE 34Bus test system is an unbalanced distribution system. The system consists of 34 nodes interconnected by 34 lines and the test system data is provided in [27]. The FV analysis results in a matrix and is extracted with the proposed method in a DIGSILENT environment as indicated in Figure 10.

All the optimization parameters of BSFLA are standardized where number of frogs, P; number of *memeplexes* mp; number of frogs in each *memeplex*, nf; number of generation for each *memeplex* before shuffling g; number of shuffling iterations; number of shuffling iterations tmax. The selected parameters are: P=60, mp=10, nf=6, g=5 and tmax=50 respectively. In this paper, the best values for the aforementioned parameters are obtained by running the BSFLA algorithm 100 times.
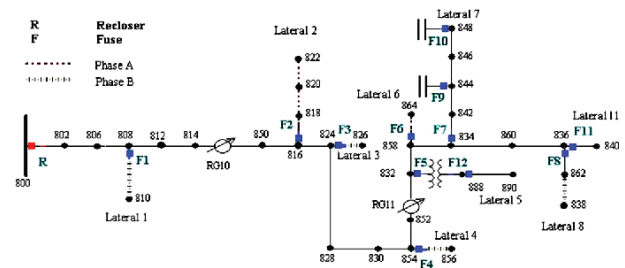

Figure 9. Implementation of BSFLA for optimal PQM placement

Figure 10. Short circuit analysis in the DIGSILENT environment to form FV matrix

Table 1 shows the optimal number of PQMs and the computational times in the IEEE 34BUS system at different α values by BSFLA and are compared with QBPSO and AQBPSO by [20] to validate the optimal solutions. As can be seen in this table, in terms of computational time, the BSFLA is faster than the QBPSO

Table 1. The optimal number of PQMs and elapsed time on 34Bus system at different α values

α value	BSFLA		QBPSO [20]		AQBPSO [20]	
	Number PQMs	Elapsed Time(s)	Number PQMs	Elapsed Time(s)	Number PQMs	Elapsed Time(s)
0.85	3	1.521	3	1.15	3	2.723
0.75	3	1.742	3	1.39	3	2.782
0.65	4	2.107	4	1.63	4	2.762
0.55	5	2.222	5	3.09	5	3.265
0.45	6	2.413	6	4.38	6	3.513
0.35	8	2.541	8	17.13	8	3.786
0.25	9	2.742	9	87.47	9	3.878

Table 2. The optimal arrangement of PQMs with optimal fitness values at different α values

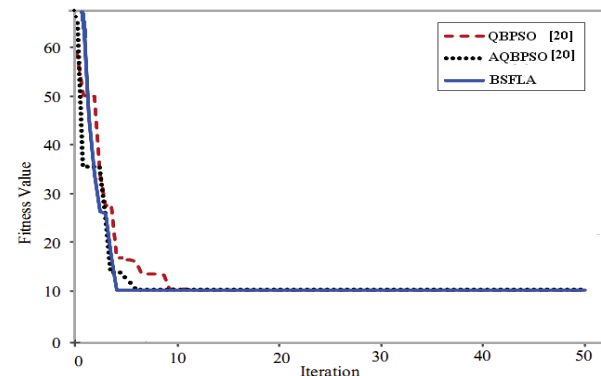| α	BSFLA		QBPSO [20]		AQBPSO [20]	
	Placement (bus) of PQMs	Average Fitness value	Placement (bus) of PQMs	Average Fitness value	Placement (bus) of PQMs	Average Fitness value
0.85	800, 808, 832	10.18	800, 808, 832	N.R	800, 808, 832	N.R
0.75	800, 812, 846	11.54	800, 812, 846	N.R	800, 812, 846	N.R
0.65	800, 808, 814, 888	12.98	800, 808, 814, 888	N.R	800, 808, 814, 888	N.R
0.55	800, 808, 814, 852, 890	14.72	800, 808, 814, 852, 890	N.R	800, 808, 814, 852, 890	N.R
0.45	800, 808, 812, 832,850, 890	16.76	800, 808, 812, 832,850, 890	N.R	800, 808, 812, 832, 850, 890	N.R
0.35	800, 808, 812, 822, 848, 850, 854, 890	17.18	800, 808, 812, 822, 848, 850, 854, 890	N.R	800, 808, 812, 822, 848, 850, 854, 890	N.R
0.25	800,808,814,822, 832, 848, 850, 854, 890	21.62	N.R	23.16	N.R	23.01

Table 3. Performance of BSFLA and other references on 34Bus system for α at 0.25 P.U

Item		Worst	Average	Best	Standard deviation
BSFLA	Fitness	21.65	21.62	21.58	0.241
	Iteration	83	13.43	6	13.89
	Time (s)	3.121	2.887	2.742	0.265
QBPSO [20]	Fitness	26.10	23.16	23.01	0.692
	Iteration	30	13.15	8	5.669
	Time (s)	182.03	111.98	76.35	34.59
AQBPSO [20]	Fitness	23.01	23.01	23.01	0.000
	Iteration	72	15.85	7	13.89
	Time (s)	3.991	3.956	3.896	0.210

Figure 11. The best performance characteristics of BSFLA, AQBPSO and QBPSO in solving PQM placement for 34Bus system when $\alpha = 0.85$

and as well as AQBPSO as the α value decreases. Although for the α value greater than 0.55 per unit, the computational times by QBPSO and AQBPSO are comparable; however by decreasing the α value, the computational times by BSFLA is uniformity increased.

Table 2 shows the optimal PQM placement at optimal buses of the system of BSFLA with related optimal fitness value, and finally, results are compared with AQBPSO and QBPSO by [20] to validate the result. The results showed that the bus locations for placing the PQMs in the 34Bus system are nearly similar for BSFLA and both AQBPSO and QBPSO.

The term 'N.R' in Table 2 means that the corresponding value is not reported by that reference. Table 3 shows the performances of various algorithms in terms of convergence rate and quality of solution after performing 20 runs at α = 0.25. As can be seen in the Table, all methods have obtained a same optimal solution. However, BSFLA shows good optimal solution in average and more accurate based on range of suboptimal solutions between the best and the worst values as indicated by the average values in compared with AQBPSO and QBPSO by [20]. Based on the standard deviation (σ), all of the algorithms provide a precise solution. In terms of computational times, BSFLA is faster than AQBPSO and is much faster than QBPSO. The result has also illustrated that BSFLA converge faster than AQBPSO and QBPSO in which it has solved the optimization problem in 6 iterations compared to the AQBPSO in 7 iterations and QBPSO in 8 iterations.

Table 4. Fault detection by the suggested PQM

Number of PQM detecting fault				Total	Accuracy
α	No PQM	1 PQM	2 PQM	3 PQM		
0.75	0	5	75	20	100	100%
0.85	2	8	80	10	100	98%

Figure 11 shows the best characteristic of each algorithm in obtaining optimal solution for the IEEE 34Bus system when α = 0.85. According to this figure, BSFLA has demonstrated a faster convergence than the AQBPSO whereas QBPSO gives the worst performance in terms of convergence rate. Although, AQBPSO does not converge fast, it has provided a better optimal solution in average as compared to QBPSO.

Hence, BSFLA has shown the best performance of the optimization techniques, but it does not show a significant different between them since the best obtained fitness values are same, and it requires to test on large scale systems.

In order to further validate the placement, 100 faults at different locations are randomly simulated. From all 100 simulated faults, 60% single phase faults, 30% two phase faults and 10% three phase faults are considered. The PQMs will be triggered if one of the phase voltage magnitudes drops down to the threshold level 0.75, and the event will be recorded by the particular PQM. Table 4 shows a summary of the fault detection activity by 3 PQMs at the suggested locations. According to the table, for α = 0.75, all the simulated faults are detected and recorded by at least 1 PQM. In other words, referring to the results in Table 4, for alpha equals 0.75, no voltage sag was incorrectly monitored, whereas for alpha equals 0.85, 5 two voltage sags were incorrectly monitored. For the voltage sags monitored by three PQMs, 20 faults that resulted in voltage sags were monitored more than once at $\alpha = 0.75$, whereas 10 faults were monitored at $\alpha = 0.85$. However, a more accurate PQM monitoring of voltage sags is achieved at $\alpha = 0.75$ compared with $\alpha = 0.85$. Thus, it is proven that the obtained PQM placements are capable of observing and capturing any fault occurrence in the whole system.

7. Conclusion

In this paper, due to the discrete binary search space nature for PQMs placement, in which every position vector can take only 0 or 1, the binary version of the shuffled frog-leaping algorithm, BSFLA-based method, was introduced. The absolute "tanh" transformation to the component of the absolute jump is presented and squashes absolute jump into the range of [0, 1]. The objective function base on the minimum number of PQMs, along with the minimizing monitor overlapping index and the maximizing sag severity index, is formulated and optimized using BSFLA. In this paper, the results of short circuit analysis using DIGSILENT software are imported to the optimization media that is handled by BSFLA. The algorithm was applied to IEEE 34BUS unbalanced distribution system. For different voltage sag thresholds, the optimal

number and configuration, as well as the MOI and SSI indices, are analyzed. The effect of the threshold of the voltage sags on the MOI and SSI indices are evaluated. Thus, the lower the threshold of the voltage sags, the smaller the MOI and the higher the number of monitors required, which avoids overlapping in the monitoring scheme. When the voltage threshold reduces from 0.85 to 0.25, the MOI index decreases from 1.132 to 1.004.

Also Fitness values, convergence time and iteration numbers are determined and compared with QBPSO and AQBPSO, which were utilized in previous studies. Results depict that BSFLA produces the best solution compared to the other optimization methods. Other advantages of BSFLA include fast convergence, small run time, capability of finding global optimum and nearly zero standard deviation.

AUTHORS

Ashkan Doust Mohammadi – Department of Electrical Engineering, Borujerd Branch, Islamic Azad University, Borujerd, Iran, e-mail: ashkan.doustmohammadi@gmail.com.

Mohammad Mohammadi[*] – Department of Electrical Engineering, Borujerd Branch, Islamic Azad University, Borujerd, Iran, e-mail: mohammadi.m.84@gmail.com.

[*]Corresponding author

References

[1] A. Rohani, M. Abasi, A. Beigzadeh, M. Joorabian, and G. B. Gharehpetian. "Bi-level power management strategy in harmonic-polluted active distribution network including virtual power plants," *IET Renewable Power Generation*, vol. 15, no. 2, pp. 462–476, 2021, doi: 10.1049/rpg2.12044.

[2] A. Kazemi, A. Mohamed, H. Shareef, and H. Zayandehroodi. "A review of power quality monitor placement methods in transmission and distribution systems," *Przegl¹d elektrotechniczny*, vol. 89, no. 3 A, pp. 185–188, 2013.

[3] D. J. Won, I. Y. Chung, J. M. Kim, S. I. Moon, J. C. Seo, and J. W. Choe. "A new algorithm to locate power-quality event source with improved realization of distributed monitoring scheme," *IEEE transactions on power delivery*, vol. 21, no. 3, pp. 1641–1647, 2006, doi: 10.1109/TPWRD.2005.858810.

[4] D. J. Won and S. I. Moon. "Optimal Number and Locations of Power Quality Monitors Considering System Topology," *IEEE transactions on power delivery*, vol. 23, no. 1, pp. 288–295, 2008, doi: 10.1109/TPWRD.2007.911126.

[5] M. A. Eldery, E. F. El-Saadany, M. M. A. Salama, and A. Vannelli. "A novel power quality monitoring allocation algorithm," *IEEE transactions on power delivery*, vol. 21, no. 2, pp. 768–777, 2006, doi: 10.1109/TPWRD.2005.864045.

[6] N. N. Kuzjurin. "Combinatorial problems of packing and covering and related problems of integer linear programming," *Journal of mathematical sciences (New York, N.Y.)*, vol. 108, no. 1, pp. 1–48, 2002, doi: 10.1023/A:1012778715468.

[7] M. A. Eldery, F. El-Saadany, and M. M. A. Salama. "Optimum number and location of power quality monitors," in *2004 11th International Conference on Harmonics and Quality of Power (IEEE Cat. No.04EX951)*, Sep. 2004, pp. 50–57. doi: 10.1109/ICHQP.2004.1409328.

[8] A. Kazemi, A. Mohamed, and H. Shareef. "A new power quality monitor placement method using the multivariable regression model and statistical indices," *INTERNATIONAL REVIEW OF ELECTRICAL ENGINEERING-IREE*, vol. 6, no. 5, pp. 2530–2536, 2011.

[9] A. Kazemi, A. Mohamed, and H. Shareef. "A novel PQM placement method using Cp and Rp statistical indices for power transmission and distribution networks," in *2012 IEEE International Power Engineering and Optimization Conference Melaka, Malaysia*, Jun. 2012, pp. 102–107. doi: 10.1109/PEOCO.2012.6230843.

[10] A. Kazemi, A. Mohamed, H. Shareef, and H. Zayandehroodi. "An improved power quality monitor placement method using MVR model and combine Cp and Rp statistical indices," *Przegl^{1}d elektrotechniczny*, vol. 88, no. 8, pp. 205–209, 2012.

[11] A. Kazemi, A. Mohamed, H. Shareef, and H. Zayandehroodi. "Optimal power quality monitor placement using genetic algorithm and Mallow's Cp," *International journal of electrical power & energy systems*, vol. 53, no. 1, pp. 564–575, 2013, doi: 10.1016/j.ijepes.2013.05.026.

[12] A. Kazemi, A. Mohamed, H. Shareef, and H. Raihi. "Optimal Power Quality Monitor Placement Using GACp Method for Distribution Network," 2013. Accessed: Jan. 17, 2024. [Online]. Available: https://www.semanticscholar.org/paper/Optimal-Power-Quality-Monitor-Placement-Using-GACp-Kazemi-Mohamed/d69169ce58deabed3ff868c3bb5e70a11038797b.

[13] G. Olguin and M. H. J. Bollen. "Optimal dips monitoring program for characterization of transmission system," in *2003 IEEE Power Engineering Society General Meeting (IEEE Cat. No.03CH37491)*, Jul. 2003, pp. 2484-2490 Vol. 4. doi: 10.1109/PES.2003.1271033.

[14] A. A. Ibrahim, A. Mohamed, H. Shareef, and S. P. Ghoshal. "Optimal placement of voltage sag monitors based on monitor reach area and sag severity index," in *2010 IEEE Student Conference on Research and Development (SCOReD)*, Dec. 2010, pp. 467–470. doi: 10.1109/SCORED.2010.5704055.

[15] M. Haghbin and E. Farjah. "Optimal placement of monitors in transmission systems using fuzzy boundaries for voltage sag assessment," in *2009 IEEE Bucharest PowerTech*, Jun. 2009, pp. 1–6. doi: 10.1109/PTC.2009.5281883.

[16] W. Hong, L. Dan, H. Wenqing, and D. Yuxing. "Optimal allocation of power quality monitors based on an improved adaptive genetic algorithm," presented at the 2015 Joint International Mechanical, Electronic and Information Technology Conference (JIMET-15), Atlantis Press, Dec. 2015, pp. 774–785. doi: 10.2991/jimet-15.2015.145.

[17] A. A. Ibrahim, A. Mohamed, and H. Shareef. "Optimal placement of power quality monitors in distribution systems using the topological monitor reach area," in *2011 IEEE International Electric Machines & Drives Conference (IEMDC)*, May 2011, pp. 394–399. doi: 10.1109/IEMDC.2011.5994627.

[18] A. A. Ibrahim, A. Mohamed, H. Shareef, and S. P. Ghoshal. "Optimal power quality monitor placement in power systems based on particle swarm optimization and artificial immune system," in *2011 3rd Conference on Data Mining and Optimization (DMO)*, Jun. 2011, pp. 141–145. doi: 10.1109/DMO.2011.5976518.

[19] A. A. Ibrahim, A. Mohamed, H. Shareef, and S. P. Ghoshal. "An effective power quality monitor placement method utilizing quantum-inspired particle swarm optimization," in *Proceedings of the 2011 International Conference on Electrical Engineering and Informatics*, Jul. 2011, pp. 1–6. doi: 10.1109/ICEEI.2011.6021845.

[20] A. A. Ibrahim, A. Mohamed, and H. Shareef. "A novel power quality monitor placement method using adaptive quantum-inspired binary particle swarm optimization," *Renewable Energy and Power Quality Journal*, vol. 1, no. 10, pp. 50–56, Apr. 2012, doi: 10.24084/repqj10.212.

[21] M. Abasi, A. T. Farsani, A. Rohani, and M. A. Shiran. "Improving Differential Relay Performance during Cross-Country Fault Using a Fuzzy Logic-based Control Algorithm," in *2019 5th Conference on Knowledge Based Engineering and Innovation (KBEI)*, Feb. 2019, pp. 193–199. doi: 10.1109/KBEI.2019.8734991.

[22] G. Olguin, F. Vuinovich, and M. H. J. Bollen. "An optimal monitoring program for obtaining Voltage sag system indexes," *IEEE Transactions on Power Systems*, vol. 21, no. 1, pp. 378–384, Feb. 2006, doi: 10.1109/TPWRS.2005.857837.

[23] A. A. Ibrahim, A. Mohamed, H. Shareef, and S. P. Ghoshal. "A new approach for optimal power quality monitor placement in power system considering system topology," *Przegl^{1}d elektrotechniczny*, vol. 88, no. 9 A, pp. 272–276, 2012.

[24] M. Eusuff, K. Lansey, and F. Pasha. "Shuffled frog-leaping algorithm: a memetic meta-heuristic for discrete optimization," *Engineering Optimization*, vol. 38, no. 2, pp. 129–154, Mar. 2006, doi: 10.1080/03052150500384759.

[25] M. M. Eusuff and K. E. Lansey. "Optimization of Water Distribution Network Design Using the Shuffled Frog Leaping Algorithm," *Journal of Water Resources Planning and Management*, vol. 129, no. 3, pp. 210–225, May 2003, doi: 10.1061/(ASCE)0733-9496(2003)129:3(210).

[26] M. Barati and M. M. Farsangi. "Solving unit commitment problem by a binary shuffled frog leaping algorithm," *IET Generation, Transmission & Distribution*, vol. 8, no. 6, pp. 1050–1060, 2014, doi: 10.1049/iet-gtd.2013.0436.

[27] U.H.Ramadhani, R. Fachrizal, M.Shepero, J.Munkhammar and J.Widen. "Probabilistic load flow analysis of electric vehicle smart charging in unbalanced LV distribution systems with residential photovoltaic generation," Sustainable Cities and Society, vol. 72, Sep. 2021, 103043, doi: 10.1016/j.scs.2021.103043.